Natural Resources Canada | Ressources naturelles Canada

GEOLOGICAL SURVEY OF CANADA
OPEN FILE 8856

Forecasting of GIC indices for Canadian power utilities

L. Trichtchenko and L. Nikitina

2022

Canada

GEOLOGICAL SURVEY OF CANADA
OPEN FILE 8856

Forecasting of GIC indices for Canadian power utilities

L. Trichtchenko and L. Nikitina

2022

Permanent link: https://doi.org/10.4095/329423

This publication is available for free download through GEOSCAN (https://geoscan.nrcan.gc.ca/).

Recommended citation
Trichtchenko, L., and Nikitina, L., 2022. Forecasting of GIC indices for Canadian power utilities; Geological Survey of Canada, Open File 8856, 27 p. https://doi.org/10.4095/329423

Publications in this series have not been edited; they are released as submitted by the author.

Table of Contents

1.Introduction

One of the most detrimental impacts of space weather events on critical technology is the impact of geomagnetic storms on the operation of electrical power systems. Depending on the severity of the geomagnetic storm (often referred as a Geomagnetic Disturbance, GMD), significant geomagnetically induced currents (GIC) can be produced in power networks, which results in multiple negative effects, ranging from voltage fluctuations, to power blackouts, to damage to transformers (see, for example, Molinski, 2002; Guillon et al., 2016).

Concern that an extreme geomagnetic storm could seriously affect power systems across North America has prompted the North American Electric Reliability Corporation (NERC) to develop new standards that require power utilities to conduct a geomagnetic hazard assessment and take appropriate mitigation measures if necessary (NERC Implementation Plan, 2018).

The best way to be prepared for a GMD event is to have a real-time forecasting system capable of predicting geomagnetically induced currents (GIC) in the system.

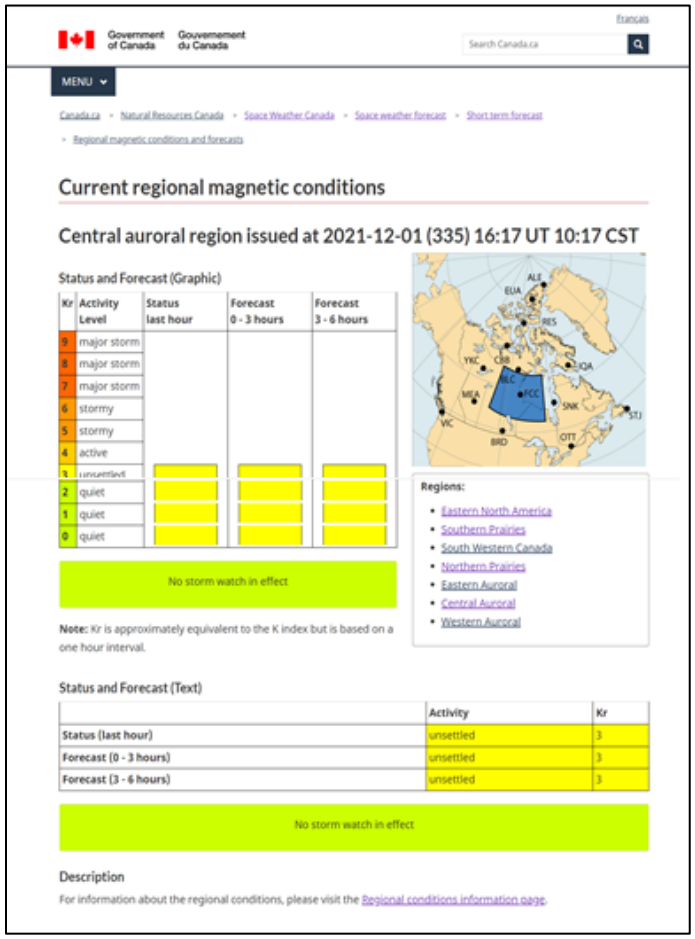

Figure 1. Example of the geomagnetic forecast for Central auroral Region produced by the Geomagnetic Laboratory/Canadian Space Weather Forecast Centre, NRCan. https://www.spaceweather.gc.ca/forecast-prevision/short-court/regional/sr-en.php

Geomagnetically induced currents in ground networks are driven by the geoelectric field, which is not usually recorded in real time at or near the network location. Thus, to forecast GIC, the first step is to forecast geoelectric field variations. It should be noted that neither a forecast of the geoelectric field, nor a forecast of GIC has ever been previously provided by any space weather forecast centre.

The Canadian Space Weather Forecast Centre / Geomagnetic Observatory operated by Natural Resources Canada provides a forecast of the ground geomagnetic activity on both a global (Canada-wide) and regional (province-wide) scale (Trichtchenko et al., 2009). An example of a regional geomagnetic forecast is presented in Figure 1. The geomagnetic forecast is given for the local hourly geomagnetic range index. The hourly range index is the difference between the maximum and minimum geomagnetic field values in each horizontal component (north-south and east-west). The forecast is providing only one value, which is the largest hourly range value for each hour among two hourly range indices of the horizontal components of the geomagnetic field.

For the power system it has been established that the hourly GIC-index (maximum GIC within an hour) correlates well (up to 93%) with the hourly range geomagnetic index (Trichtchenko and Boteler, 2004). As well, it has been identified that it is possible to use a local geomagnetic index for the GIC forecasts at a specific power grid (Trichtchenko and Boteler, 2006). Figure 2 shows the results of this study for two different GIC recording sites located in different power grids.
In this figure, the black lines in both plots represent the best fit (middle line) and two standard deviations (SD) from the best fit (top and bottom lines), obtained with use of GIC data and geomagnetic data recorded during several geomagnetic storms. New GIC data, obtained during new geomagnetic storms, not used in linear fit derivation, are plotted as color dots on top of these three lines. It is clearly seen that most of new values are located inside the two SD lines, although not centered around the best fit, due to the limited data quantity used for the linear fit (see Trichtchenko and Boteler, 2006).

Thus, if the linear fit between hourly maximum GIC index and hourly geomagnetic index is known from some statistical study, the GIC indices can be predicted based on predicted geomagnetic hourly indices.

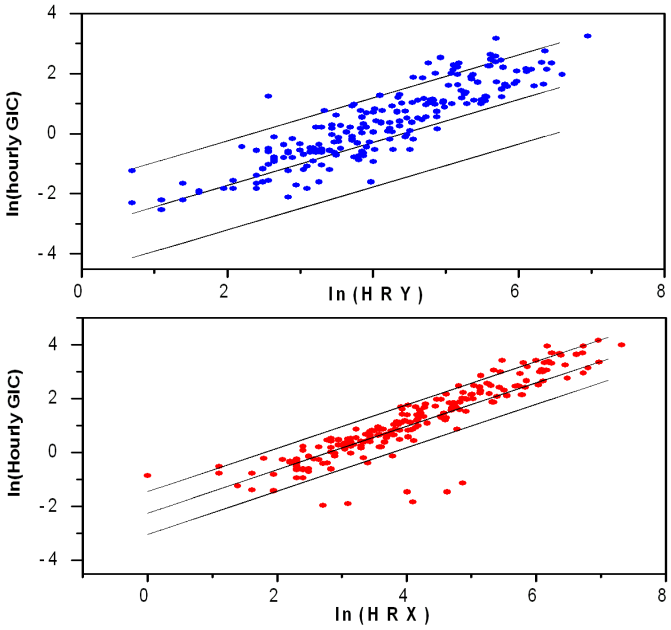

Figure 2. Verification of the linear fit predictions of the GIC indices from previously known relationships (black lines) by adding data points from events not included in the linear fit procedure (colour dots). HRX and HRY are hourly ranges of X (north-south) and Y (east-west) components of the geomagnetic field. See Trichtchenko and Boteler, 2006 for more details.

GIC are driven by the geoelectric field, and therefore, geoelectric field indices could also be predicted with use of the geomagnetic forecast.
The forecast of the geomagnetic hourly range indices can be further developed into a forecast of the geoelectric field (hourly maximum indices) and GIC (hourly maximum indices). The steps in the development and results of the forecast are presented in this Open File. Part 2 describes the logic model, Part 3 explains data generation, Part 4 presents the equations used in the model, Part 5 shows the steps for generating a forecast and Part 6 explains the forecast evaluation. Part 7 summarises the findings.

2.Logic Model

Two different approaches are used for forecasting. The first approach is to utilize the existing forecast of the magnetic hourly range indices (HRH) to forecast the geoelectric indices (hourly maximum HME), and then derive the hourly maximum GIC indices (H_GIC) at each substation of the power network. The second approach is to first directly forecast the geoelectric field indices HME, and then derive the GIC indices at each substation.

These schemes are presented in Figure 3a and 3b respectively.

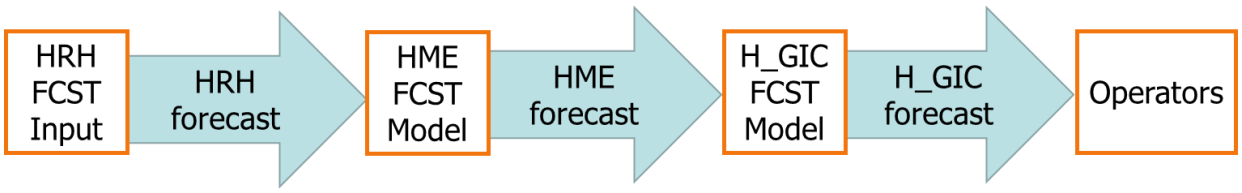

a)

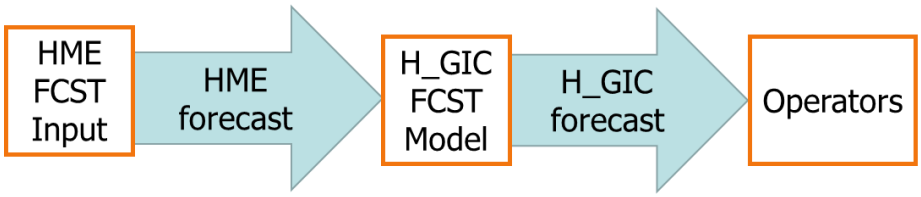

b)

Figure 3. Two different approaches to forecasting, (a) Method 1, and (b) Method 2. HRH is the geomagnetic hourly range index, HME is the geoelectric hourly maximum index, and H_GIC is the geomagnetically induced current hourly maximum, at each substation. For more detailed descriptions see the text.

For the development of the forecast based on the above two approaches, geomagnetic data, geoelectric data and the GIC data are required. While the geomagnetic data and geomagnetic indices could be directly obtained from continuous 1--min measurements of the geomagnetic field at the geomagnetic observatories operated by Natural Resources Canada, continuous recordings of the geoelectric field and continuous recordings of GIC are not available. Thus, the geoelectric field indices were obtained from the geoelectric field modelled values (1 min), calculated with use of the geomagnetic data and the earth response, derived from Earth conductivity models (Trichtchenko et al., 2019). GIC indices were obtained from GIC 1--min values, obtained from the model which uses a specific power network configuration (Horton et al., 2012) and the geoelectric field as an input. These 3 sets (i.e. geomagnetic observations, geoelectric and GIC 1--min modelled values and hourly indices based on observed geomagnetic values and electric field modelled values and GIC modelled values) are defined as “data” in this report and, generally, can be substituted by observational data if the electric field and GIC observations are available. These data are used for development of the model (generation of the regression formulae), as well as for the evaluation of the forecast.

The overall logic model, therefore, consists of three large domains:

1. Data generation
2. Model generation
3. Forecast and evaluation

as presented in Figure 4.

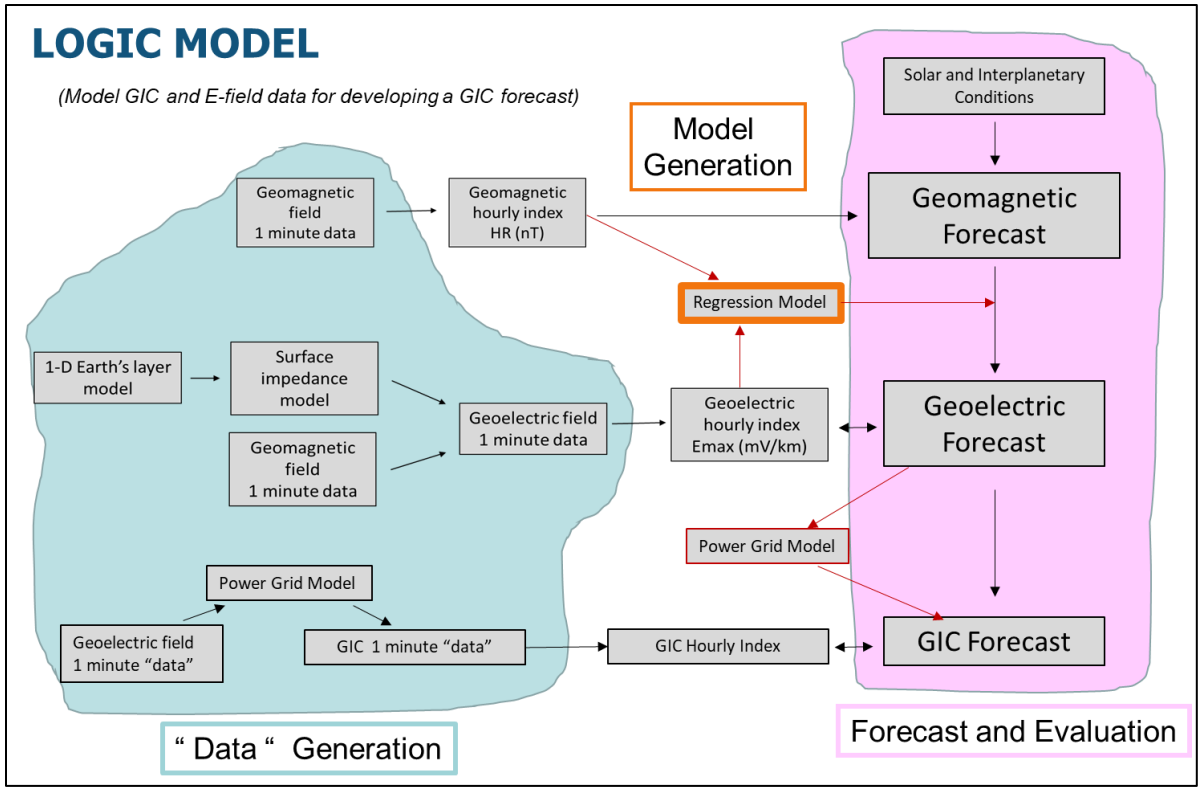

Figure 4. Logic model for the development and evaluation of GIC forecast. Three components are data generation, model generation and forecast/evaluation.

Descriptions of each domain are given in the following three Sections of the report.

3.Data Generation

3.1.Geomagnetic data and indices

Geomagnetic data can be obtained from the Natural Resources Canada on-line service https://geomag.nrcan.gc.ca/data-donnee/sd-en.php. In this study, data from geomagnetic observatories in Fort Churchill (FCC), Glenlea (GLN) and Brandon (BRD) were used. The data availability and location of observatories are presented in Table 1 and are also shown on a map (Figure 5).

Table 1. Locations of Geomagnetic Observatories

Station	Code on the map	Latitude, degrees	Longitude, degrees	Geomagnetic Latitude, 2015	Geomagnetic Longitude, 2015	Data availability (years)
Fort Churchill	FCC	58.76 N	265.9 E	67.35 N	29.69 W	1973-2015
Glenlea	GLN	49.64 N	262.9 E	58.06 N	30.63 W	1982-2006
Brandon	BRD	49.87 N	260.0 E	58.03 N	34.15 W	2007-2015

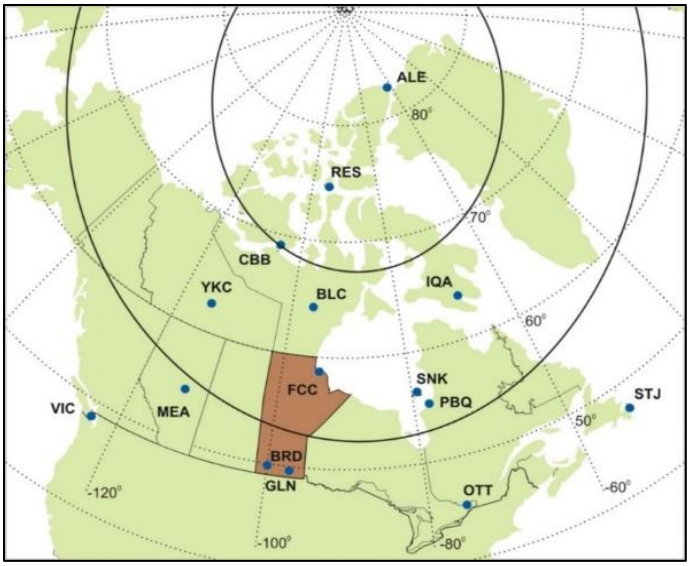

Figure 5. Map representing locations of the NRCan observatories. Solid lines identify polar, auroral and sub-auroral zones.

The geomagnetic forecast of the hourly indices HRH (nT) is based on the statistical patterns of variation of the hourly range indices during the day, separately for each month of the year (see Figure 6) with the addition of the running real-time hourly range index. In order to forecast an approximate time of a geomagnetic storm onset, information about the expected arrival of solar disturbances are also incorporated.

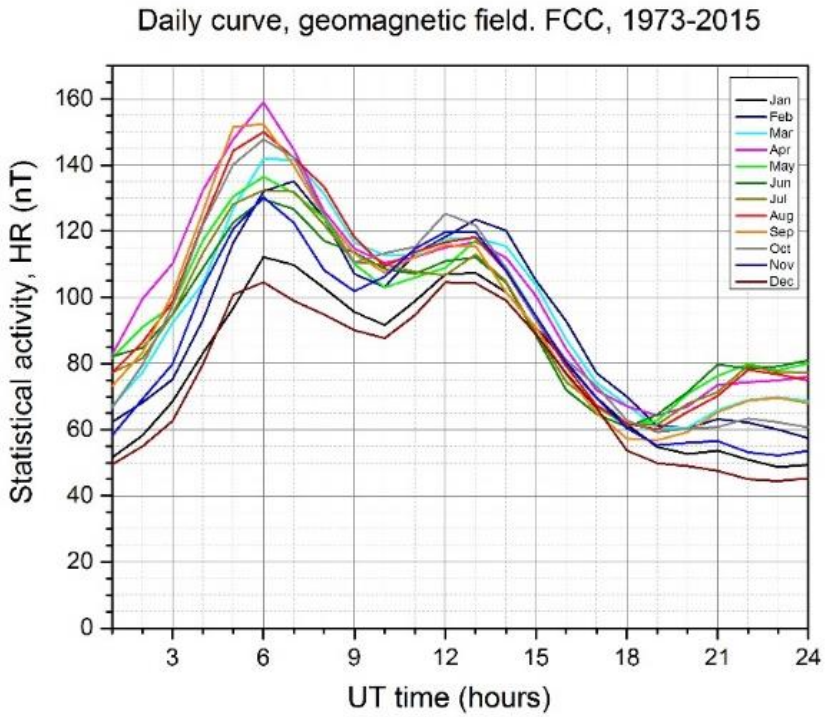

a)

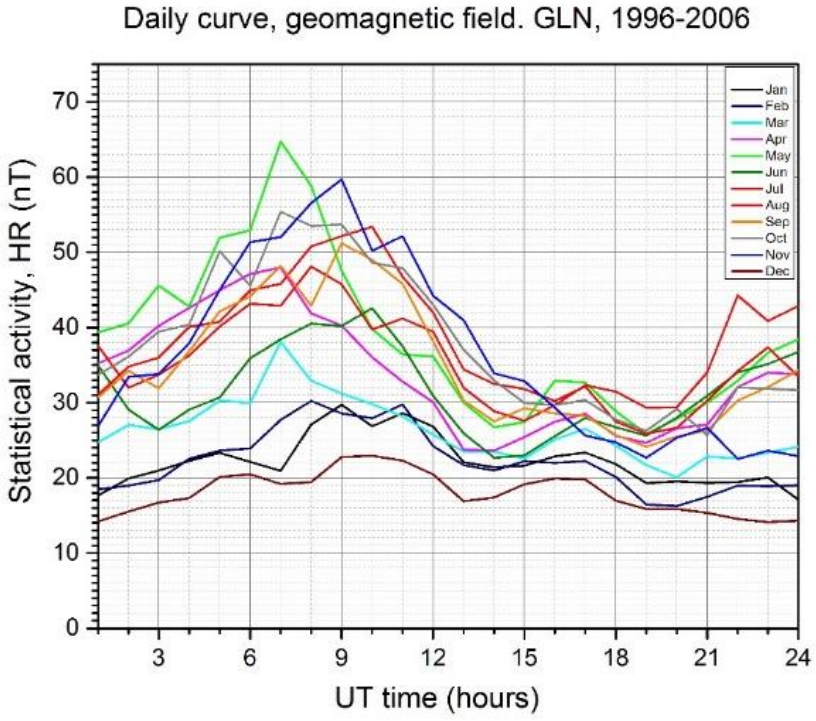

b)

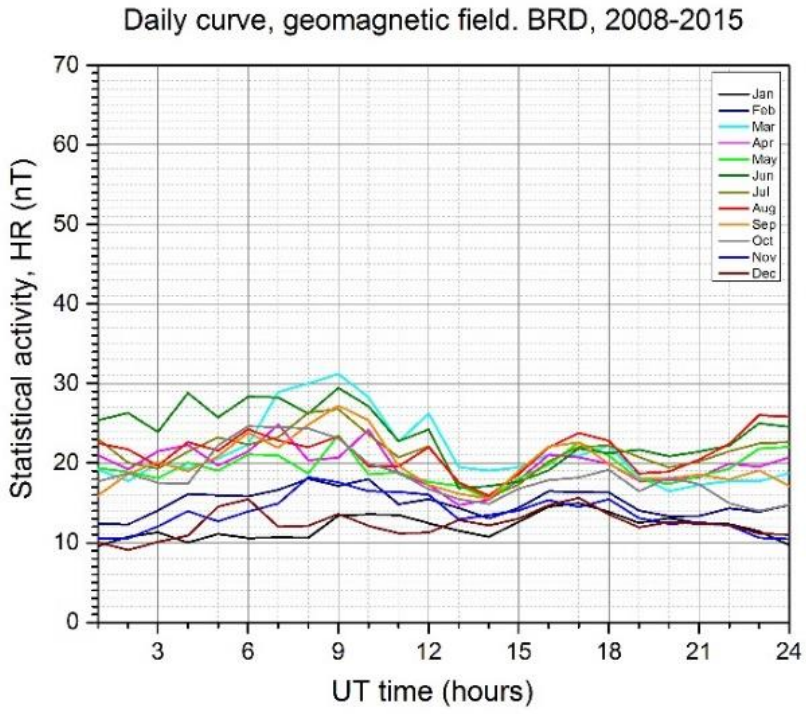

c)

Figure 6. Monthly curves of the daily mean variations of geomagnetic index at FCC (a), GLN (b) and BRD (c) observatories.

The operational geomagnetic forecast is updated automatically every 15 -mins, and provides hourly range values for the next 24 hours, for each hour, as presented in Figure 7, for each Canadian observatory. Light-grey background corresponds to conditions in the previous 48 hours, and dark grey background covers the forecast for the next 24 hours. The height of the color bars correspond to the amplitude of the hourly range in nT and their colors are corresponding to one of the 5 different levels of activity (quiet, unsettled, active, stormy, and major storm). Types of forecasts and details for the activity levels are presented at https://www.spaceweather.gc.ca/forecast-prevision/index-en.php.

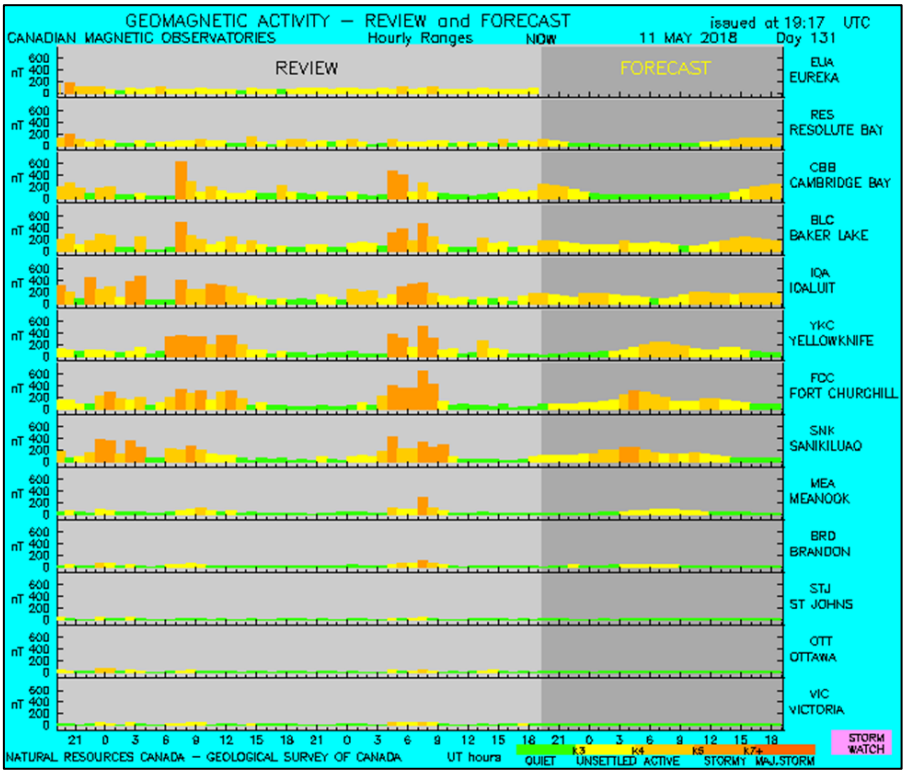

Figure 7. Example of the review and forecast of geomagnetic activity for each geomagnetic observatory. http://www.spaceweather.gc.ca/forecast-prevision/short-court/sfst-5-en.php

3.2.Geoelectric data and indices

The horizontal components of the surface electric field are obtained from the horizontal components of the geomagnetic field (Fourier-transformed to the frequency domain) multiplied by the frequency-dependent surface impedance (Simpson and Bahr, 2005, Trichtchenko et al., 2016):

$$\left[\vec{E}\ (\omega)\right] = \frac{1}{\mu_0}\left[Z_{earth}(\omega)\right]\left[\vec{B}\ (\omega)\right] \qquad (1)$$

where ω is the angular frequency, μ_0 is the magnetic permeability of free space; Vectors of electric and magnetic fields are $[\vec{E}\ (\omega)] = \begin{pmatrix} E_x(\omega) \\ E_y(\omega) \end{pmatrix}$ and $[\vec{B}\ (\omega)] = \begin{pmatrix} B_x(\omega) \\ B_y(\omega) \end{pmatrix}$

and subscripts *x* and *y* are related to the horizontal components (northward and eastward respectively). The corresponding surface impedance matrix $Z_{earth}(\omega)$ is defined by four ratios of the components of electric and magnetic fields as

$$[Z_{earth}(\omega)] = \begin{pmatrix} Z_{xx}(\omega) & Z_{xy}(\omega) \\ Z_{yx}(\omega) & Z_{yy}(\omega) \end{pmatrix} \quad (2)$$

These equations gave the frequency spectrum of the geoelectric field, and an inverse Fourier transform is performed in order to get time-domain electric field, as presented in Figure 8.

The vast majority of geoelectric field calculations for GIC applications were done using the simplest, one-dimensional Earth resistivity structure (so called "layered earth"), in which case

$$\begin{aligned} Z_{xx}(\omega) = Z_{yy}(\omega) = 0 \\ Z_{xy}(\omega) = -Z_{yx}(\omega) \end{aligned} \quad (3)$$

where the surface impedance is derived from the layered earth model by use of the recursive relations, as follows.

If the magnetic field $H_{surface}=B_{surface}/\mu_0$ at the surface of the earth (1st layer) is known from magnetic observations, the electric field can be obtained with use of the impedance at this layer Z_1, as:

$$E_{surface} = Z_1 H_{surface} \quad (4)$$

The impedance at any layer *n* can be found by applying the recursion relation for the impedance of an N - layered half-space (Weaver, 1994, p.293).

$$Z_n = i\omega\mu \left(\frac{1 - r_n e^{-2k_n d_n}}{k_n \left(1 + r_n e^{-2k_n d_n}\right)} \right) \quad (5)$$

where d_n, k_n are the thickness and propagation constants with $k_n = \sqrt{i\omega\mu_n\sigma_n}$ of the layer *n*, μ, are relative permeability (usually μ=1) and σ are conductivity of layers, and *r* is reflection coefficient defined as:

$$r_n = \frac{1 - k_n \frac{Z_{n+1}}{i\omega\mu}}{1 + k_n \frac{Z_{n+1}}{i\omega\mu}} \quad (6)$$

and for the last layer N (uniform half-space), $Z_N = \frac{i\omega\mu}{k_N}$. (7)

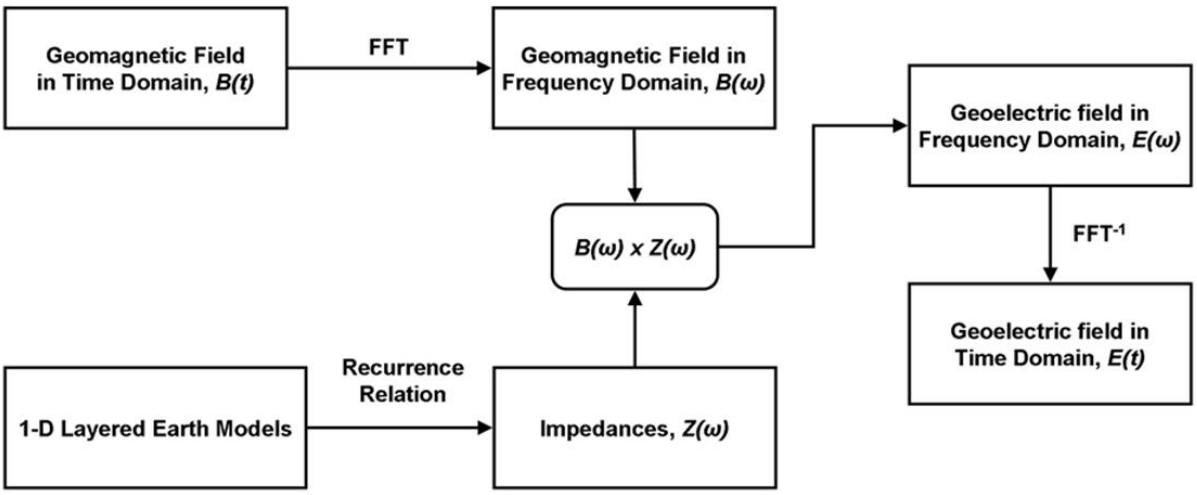

Figure 8. Schematics for calculation of the geoelectric field variations *E(t)*.

The layered earth models for all provinces of Canada can be found in Trichtchenko et al. (2019). In this report, layered Earth models for Manitoba are presented and used in further modelling (Figure 9). The map of Manitoba with colour-coded areas of different Earth's resistivity models is presented in Figure 9a, and Figure 9b presents the variations of the earth resistivity (inverse of conductivity) with the depth for each of these areas.

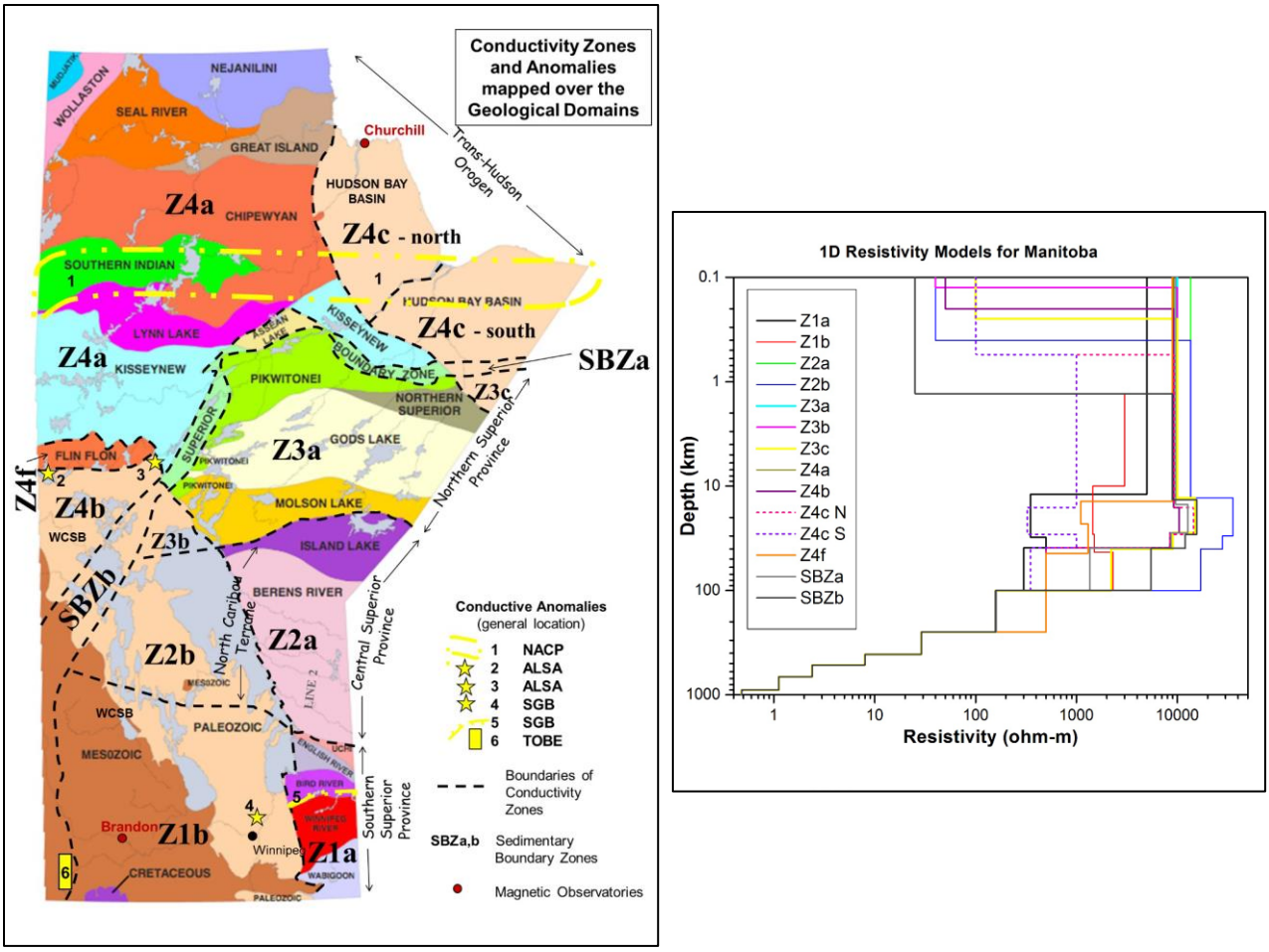

a) b)

Figure 9. Manitoba Earth resistivity models. a) Map of Manitoba with principal geological domains, conductivity zones, conductive anomalies and locations of two geomagnetic observatories (Brandon and Churchill); b) Resistivity variations for 14 different Zones (color coded) for Manitoba. Vertical scale is depth in kilometers, horizontal scale is resistivity in Ω·m.

Variations of surface impedances (amplitude and phase) with frequency are presented in Figure 10.

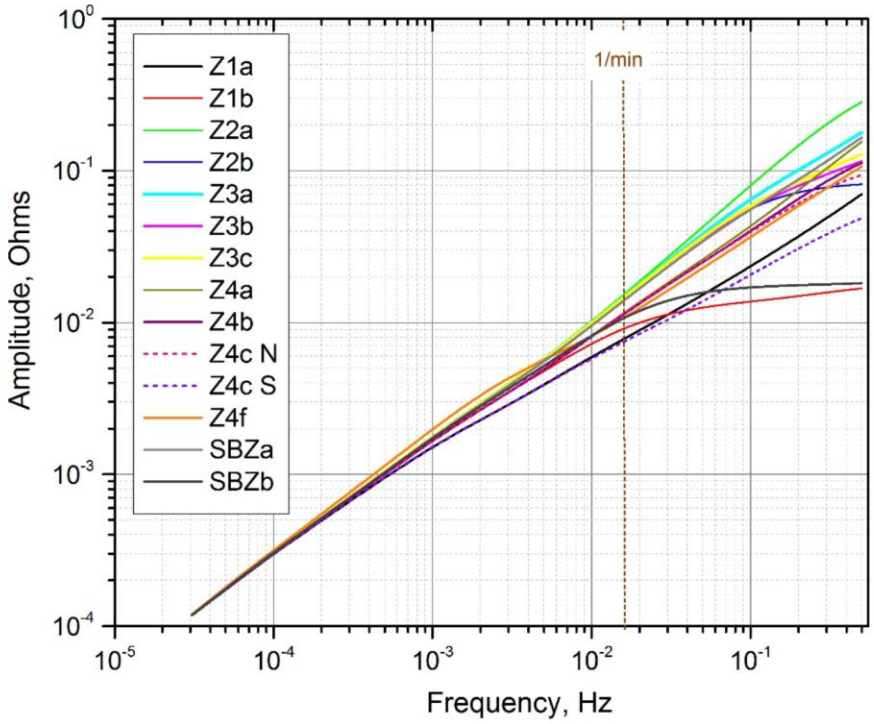

a)

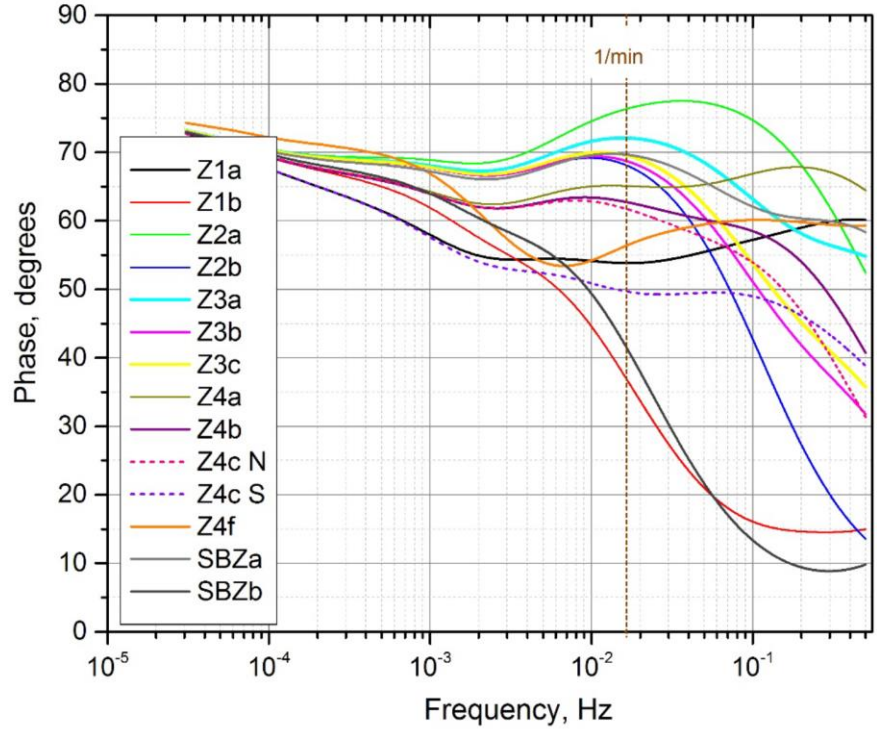

b)

Figure 10. Variations of surface impedance (a)-amplitude, and (b) phase with frequency for 14 layered Earth models of Manitoba.

The electric field (1 min values) were calculated using geomagnetic data from three geomagnetic observatories in Manitoba and the layered earth model of Zone 4f. The hourly maximum amplitude of the electric field (HME) has been chosen as an hourly index for the further derivation of the regression relations. Modelling results for mean daily HME index for each month of the year with conductivity model are presented in Figures 11 a-c for GLN and BRD observatories respectively.

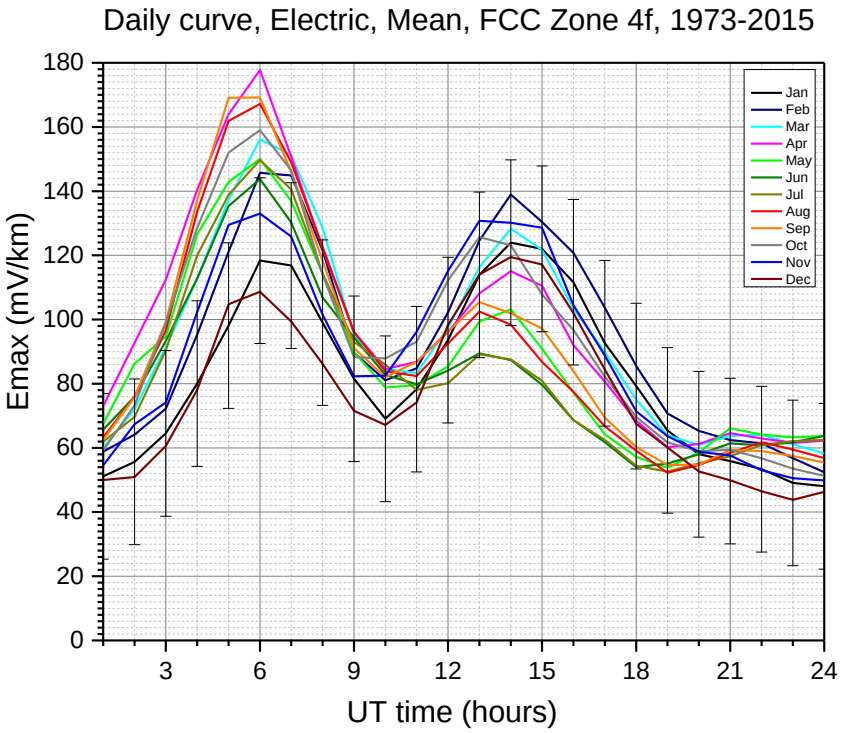

a)

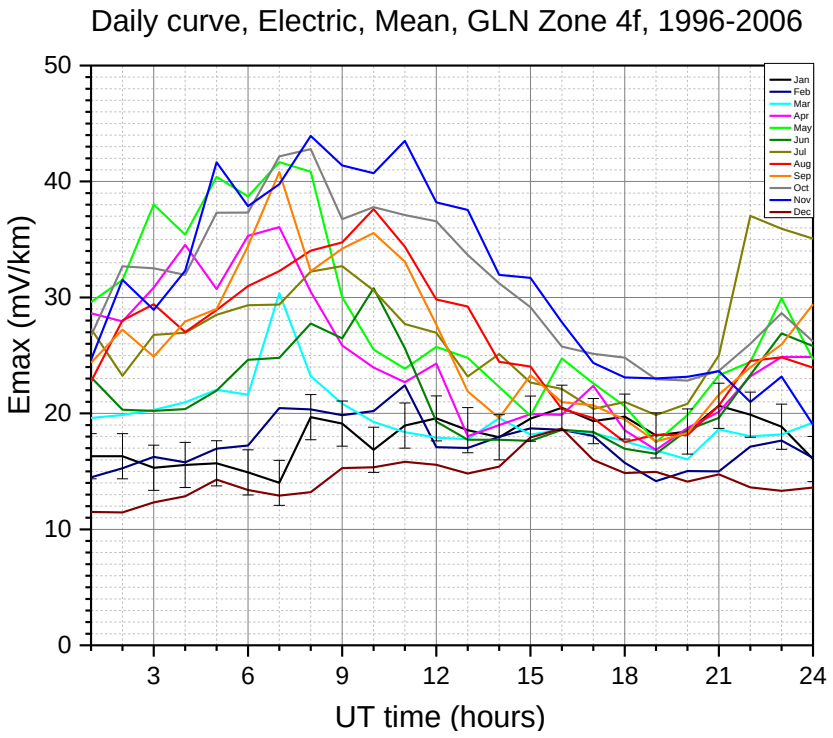

b)

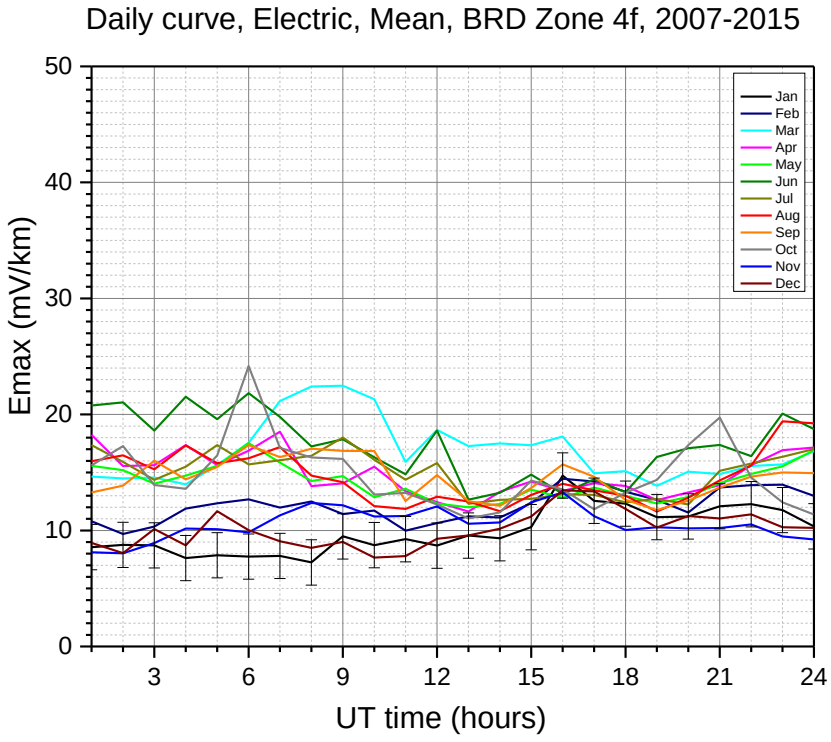

c)

Figure 11. Mean daily curves of geoelectric HME for each month averaged over all years of data availability: a) FCC, b) GLN and c) BRD. Earth conductivity model Zone 4f. Error bars are presented for January only (as an example).

The daily curves present variability of the geoelectric field which is significant in the northernmost station of FCC, less in GLN and the smallest one is in BRD. The deviation from the mean (shown as error bars) for January follow the same trend and is the largest in the FCC, less in GLN and the smallest is in BRD. Patterns of daily variability with two maxima are more coherent at FCC, and the least coherent in BRD.

3.3.GIC data and indices

As a test case, the "benchmark" network model has been used. This benchmark network scheme has been developed to include many features found in typical high voltage (HV) and extra high voltage (EHV) networks (see *R. Horton et al., 2012*) specifically for studies of the impacts of GIC on different network components. The network includes single and multiple transmission lines; the substations include both conventional transformers and autotransformers, series and neutral connected GIC blocking devices are also included in the network.
The details of the network are described in Horton et al. (2012) and are not reproduced in this report, as the purpose of the report is to present the forecasting methods and results, not to detail the network response to GIC.

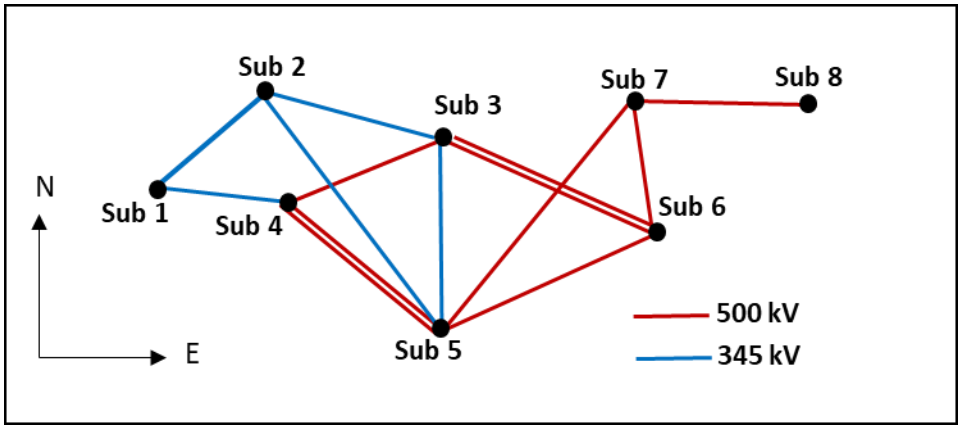

Figure 12. Schematic configuration of the benchmark network, redrawn after Norton et al, 2012

The equivalent scheme of the network is shown in Figure 12. For application purposes, the benchmark power grid has been oriented on Earth to be elongated in latitude (line Sub 7 to Sub 8 follows a line of constant latitude), and the line between Substations 5 and 3 is along the north-south direction (consistent with the calculations presented in Boteler (2013)). Results are presented for GIC in Substation 5 only.

GIC modeling in the power system requires knowledge of the resistances of the transmission lines as well as the resistances of the transformers and the grounding resistances at the substations. These resistances are then used with geoelectric field values to give the GIC in each line of the network. For demonstration of the GIC forecast, the GIC modelling in the benchmark network presented in Boteler (2013) has been used.

In general, modelling GIC starts with defining the voltage sources in each line by integrating the

geoelectric field components along the line, and then using Kirchoff's rules to obtain matrix equations for the current in each node (i.e. connection to the ground):

$$[i(t)] = [Z][V(t)] \tag{8}$$

where i(t) represents GIC in each node of the network, Z represents the network impedance and V(t) represents the voltage in each line.

Based on the principle of linear superposition (Boteler 2013), current in each node i can be obtained as a superposition of two components:

$$I_i(t) = \alpha_i E_N(t) + \beta_i E_E(t) \tag{9}$$

where the coefficients are obtained from the calculations of GIC values for 1) only northward electric field E_N = 1V/km, with no Eastward electric field E_E = 0 V/km (α-coefficient) and for the case of 2) only eastward E_E=1V/km and E_N=0 V/km (β-coefficient).

In this report, the Substation 5 will be used for calculations of the GIS -min values, hourly maximum indices and forecast of the H_GIC, with coefficients α=-279.0 and β=-65.5 (Boteler, 2013).

It should be noted, that GIC values depend on the direction of the geoelectric field. The developed forecast provides only one value of the forecast geoelectric index (hourly maximum amplitude), without direction, thus, the forecast values of H_GIC are evaluated for the worst case of electric field direction. For this, the direction of the geoelectric field in each substation is assumed to be along the direction which gives the highest GIC value.

4.Model Generation

This part describes the derivation of two regression models for estimations of the forecasted geoelectric and GIC indices based on statistical daily variabilities of the geomagnetic (approach 1) and geoelectric (approach 2) hourly indices.

4.1. Approach #1

This approach is based on the application of the regression relation between the geomagnetic hourly range index (HRH) and geoelectric hourly maximum index. Thus, the forecasted HME indices are obtained from the forecasted HRH indices. The simple liner fit of the logarithmic values of these two indices are used to demonstrate the validity of the approach:

$$\log(HME) = k \cdot \log(HRH) + \log(c) \qquad (10)$$

which transforms to the power law as

$$HME = c \cdot HRH^{k} \qquad (11)$$

Linear regression for FCC obtained with use of the geoelectric field modelling results based on geomagnetic data for year 2004 with the earth resistivity model of Zone 4 f is presented below:

$$HME = 1.05 \cdot HRH^{0.96} \qquad \ldots.(12)$$

and the corresponding plot is presented in Figure 13.

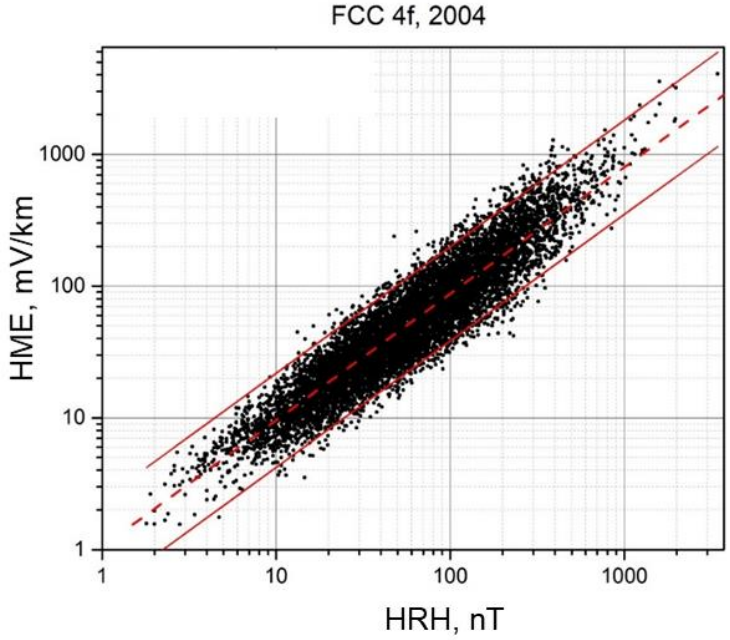

Figure 13. Geoelectric hourly index (HME, mV/km) and the corresponding geomagnetic hourly index (HRH, nT). Red lines represent: a linear fit (dashed), and a 95% confidence interval (solid); black dots are data.

4.2. Approach #2

Direct forecast of the geoelectric hourly indices directly is based on the algorithm currently used operationally for the forecast of geomagnetic hourly range indices.
The daily curves of the geoelectric hourly index HME are the core of the proposed forecast of geoelectric activity.

The forecast scheme consists of two parts, the first is calculation of the running indices (A) and the second is calculation of the forecast values of hourly indices (B).

A) Two running indices are calculated every 15 -mins:

1. the **running hourly maximum** index, ***rhE(t),*** is calculated as the maximum amplitude of -min electric field values for the last 60 -mins,

$$rhE(t) = \max(abs(E(t - 59min : t))) \quad (13)$$

.

2.the **running daily mean** of the last 24 hourly indices *rhE* abbreviated as ***rdE(t)***, is calculated as follows:

$$rdE(t) = \text{mean}\big(rhE(t - 23hr : t)\big)\,. \quad (14)$$

The above steps are presented graphically in Figure 14.

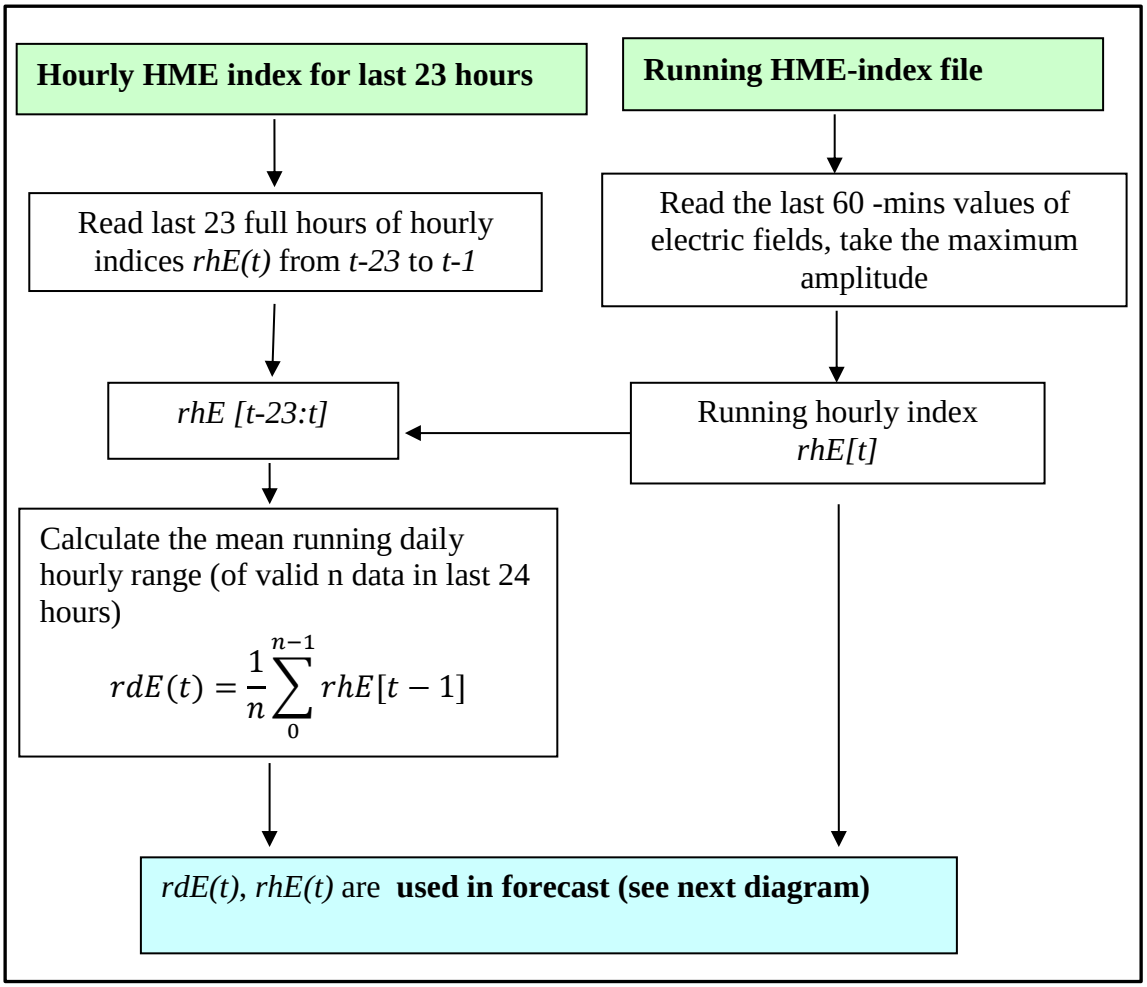

Figure 14. Steps for obtaining of the running indices.

B) Calculations of the Forecast values

1.Calculation of the basic forecast for the next 24 hours from the known normalized statistical daily curves (***d_c)*** (see Part 3.2 for examples), scaled to the latest running daily mean ***rdE(t)*** (14) as follows:

$$Forecast1[t+1:t+24\ hr] = d\_c[t+1:t+24\ hr] \cdot rdE(t)\ . \qquad (15)$$

2.Adjustment of the forecast to the conditions in the last hour with use of the running hourly value ***rhE(t)***. The adjustment term is calculated as follows:

$$Forecast\_adj(t+i) = \big(rhE(t) - rdE(t)\big) \cdot Staf \cdot Df(i) \qquad (16)$$

for $i = 1, 2, \ldots, 12\ hr$, forecast hours

where

Df is a "decrease" factor, applied to attenuate the impact of the current activity into the future, i.e. to keep the impact of current conditions decreasing during the first 12 hours:

$$Df(i) = \frac{(13-i)}{12}. \quad (17)$$

Staf is the factor specific for each geomagnetic observatory location (station factor), and can vary depending on a geomagnetic station and surface impedance model. The value for the *Staf* coefficient corresponds to the absolute minimum value among all the values in the diurnal curves of the HME indices, thus taking into account the geomagnetic variations at a specific observatory and specific surface impedance model. Station Factors (*Staf*) are presented in the Table 2 for FCC, GLN and BRD with for surface impedance Zone 4f.

3.The resulting forecast is the sum of the climatological forecast and the adjustment, as follows:

$$Forecast[t+1:t+24] = Forecast1[t+1:t+24] + Forecast\_adj[t+1:t+12] \quad (18)$$

Table 2. Station factor (*Staf*) used to forecast electric field indices

Observatory	FCC	BRD	GLN
Earth's conductivity model (Zone)	4f	4f	4f
Factor (*Staf*)	0.54	0.72	0.63

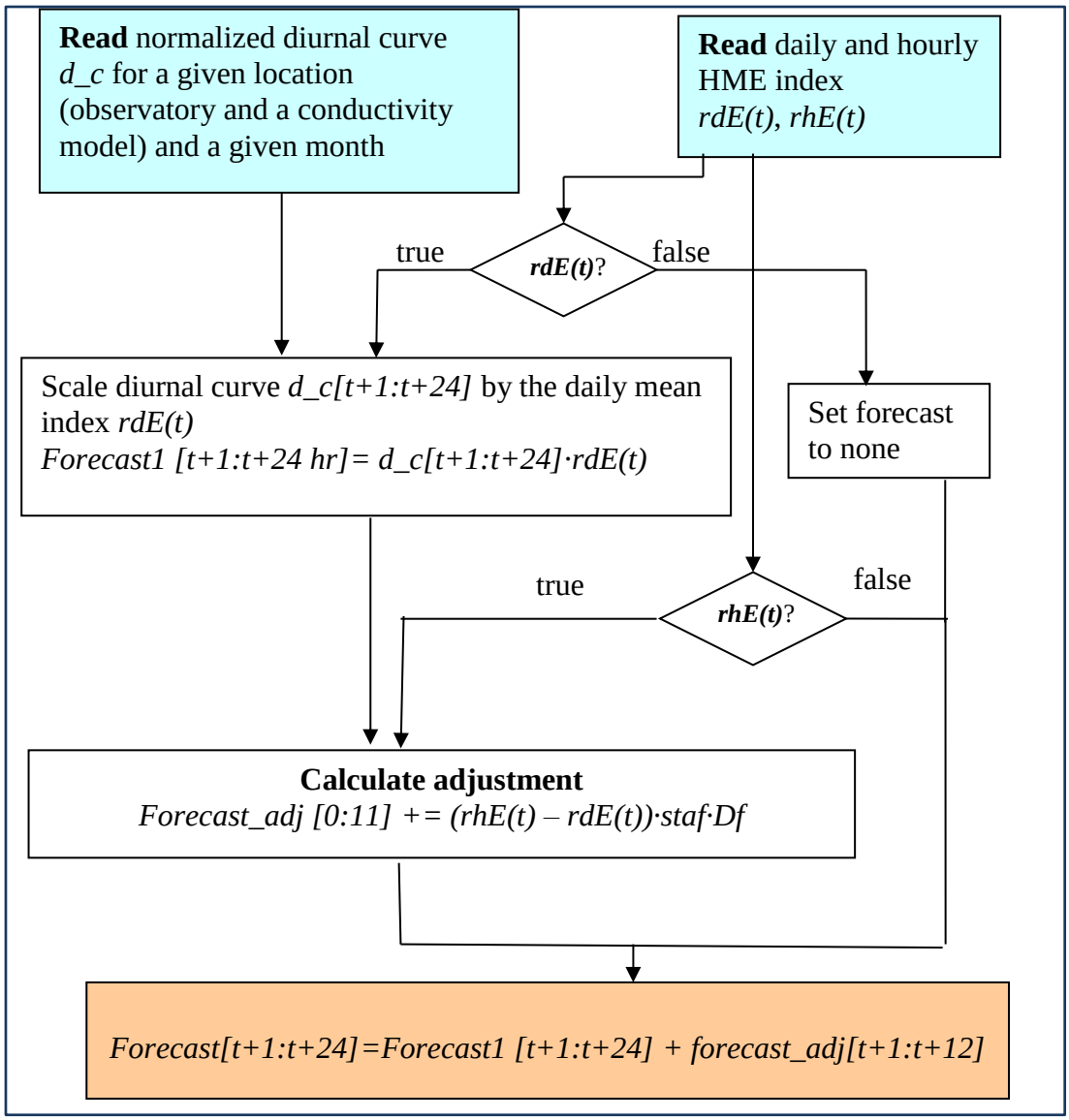

Figure 15. Forecast flowchart.

Figure 15 is a graphical representation of the steps for generating the forecast. It should be noted that there may be a case when the data are not provided due to some malfunction at the observation site. In this case the running indices might be unavailable and the forecast is not produced.

Forecast values of hourly maximum electric field amplitude (HME) and hourly maximum GIC index are provided every 15 -mins for the next 24 hours. It should be noted, that the geoelectric field hourly index is the maximum amplitude of the horizontal geoelectric field and does not provide information about the electrical field direction.

5.Forecast results and evaluation

5.1.Statistical evaluation of the forecast

The Canadian Space Weather Forecast Center describes monitored and forecast geomagnetic activity in terms of specific levels: Quiet, Unsettled, Active, Stormy, and Major Storm https://www.spaceweather.gc.ca/forecast-prevision/cond-en.php . Following this example, the activity levels for the geoelectric and GIC indices were identified as described in Table 3.

Table 3. Activity levels of the geoelectric field and GIC

Activity level	Quiet	Unsettled	Active	Stormy	Major Storm
HME(mV/km)	0-80	80-145	145-250	250-800	>800
H_GIC (A)	<50	50-100	100-200	200-400	>400

For the statistical evaluation of the forecast results, all indices (data and forecast) were binned based on these 5 activity levels.

Statistical evaluation of 2 approaches for HME forecasts (FCC, Zone 4f) and H_GIC forecast (station 5 of the benchmark network) for year 2004 are presented in Figure 16.

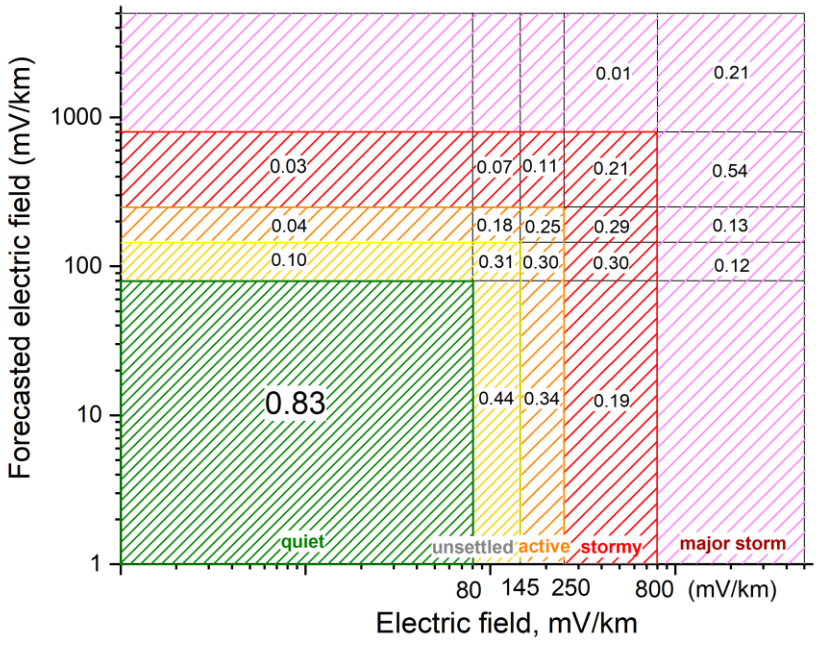

a)

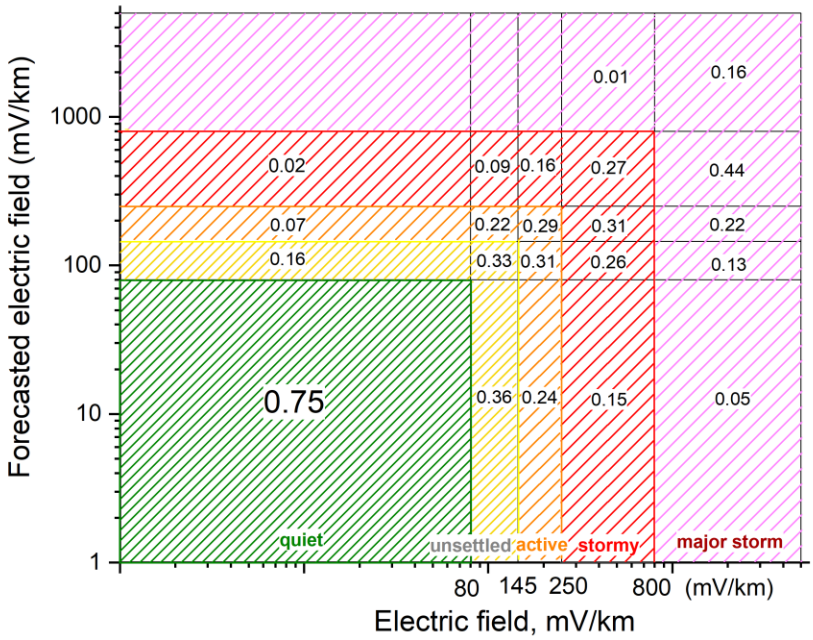

b)

Figure 16. Statistical evaluation of the 3 hour ahead forecast: a) forecast of the electric field indices HME with Approach # 1; b) forecast of the geoelectric field indices HME with Approach # 2. FCC magnetic data with the Earth's resistivity profile 4f.

The performance of the two different methods of determining the HME forecast is inferred from Figure 16. Approach #1 performs better in forecasting quiet to unsettled activity levels. For all other activity levels, the performance of Approach #1 and Approach #2 is comparable.
For more detailed performance evaluations more studies are foreseen when the proto-operational system is developed.

5.2.Forecast of GIC for the benchmark network

To demonstrate the performance of the developed forecast, consider data modelled and collected during a geomagnetic storm that occurred 07-08 November 2004. For this event, the location of the benchmark network is assumed to be near FCC with a zonal conductivity structure as in Zone 4f.
The results of the forecast of the GIC index at the Substation 6 of the benchmark network is presented in Figure 17 together with the "data" obtained from the network modelling results calculated with use of 1 min values of E_x and E_y components of the geoelectric field (grey bars on the Figure 17).

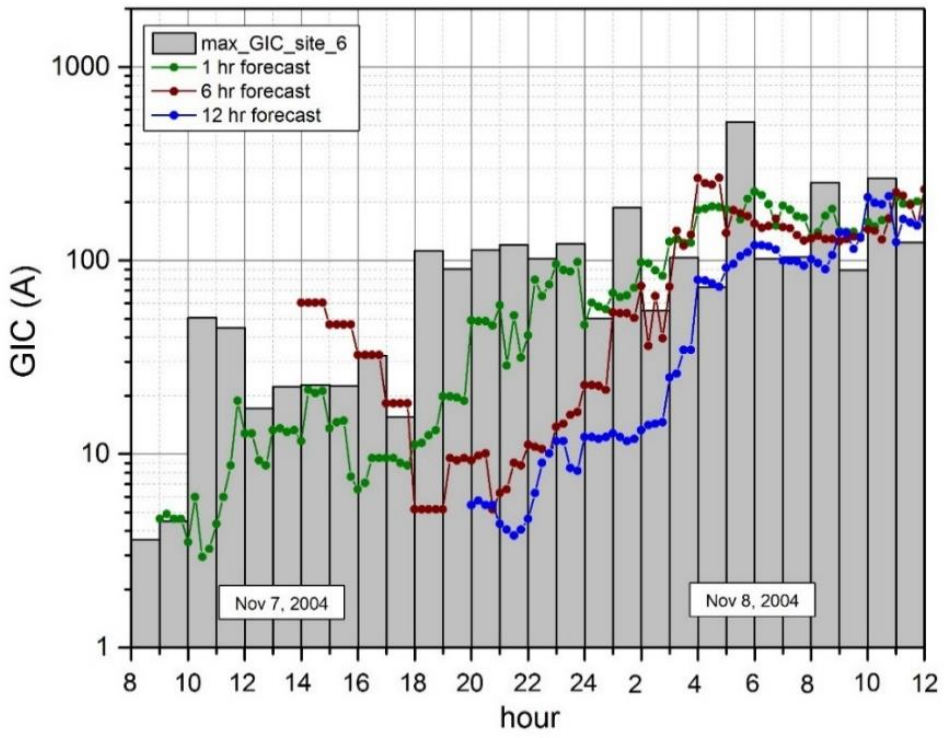

a)

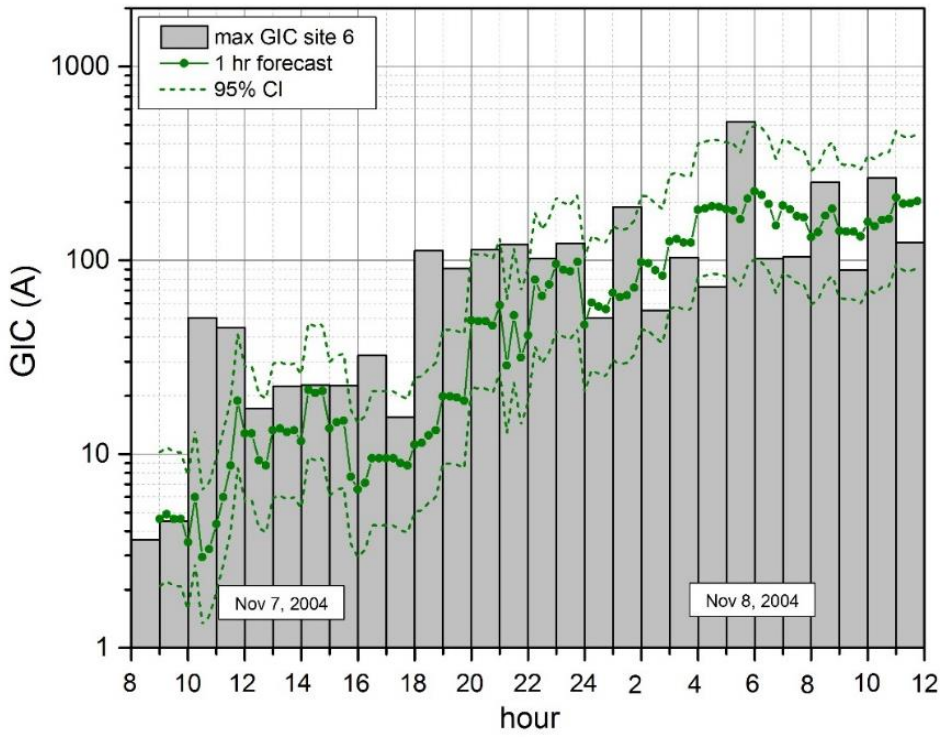

b)

Figure 17. Calculated values (grey bars) and the forecast (colored lines) of the GIC index at substation 6 of the benchmark network model: a) green curve is the 1-hr forecast, brown curve is the 6-hr forecast and blue curve is the12-hr forecast; b) 1-hr forecast GIC (solid green line) with 95 % confidence interval (dashed). Forecast is performed with use of Approach #1.

As expected, the 1-hour forecast gives the best representation of the real GIC values (Figure 17a), and it should be noted that, the 95% confidence interval covers the significant part of the GIC index variability (Figure 17b) for the period under consideration.

6.Summary

This report presents a novel method for the forecasting geoelectric field and GIC values. This research was done as part of a project together with Manitoba Hydro
Two slightly different approaches are presented, such as: 1) based on the statistical pattern of the mean daily variations of the geomagnetic field hourly index, and 2) based on the statistical pattern of the mean daily variations of the geoelectric field hourly index. The variations are averaged over many years of geomagnetic observation, and to include seasonal variations, the diurnal curves were obtained separately for each month.
The capabilities for the GIC forecast (hourly maximum indices of GIC) were demonstrated for a benchmark power grid, but can be extended for any power grid configuration, provided there are geomagnetic observatories with real-time data provision near the location of the power grid.
Further evaluation, validation and testing will be required before operational use of the developed methods.

7.References

Boteler, D.H. (2013), The use of linear superposition in modelling geomagnetically induced currents, 2013 IEEE Power & Energy Society General Meeting, Vancouver, BC, 2013, pp. 1-5. doi: 10.1109/PESMG.2013.6672717

Guillon, S., Toner, P., Gibson, L., Boteler D.H. (2016). A colorful blackout: The havoc caused by auroral electrojet generated magnetic field variations in 1989. IEEE Power and Energy Magazine, 14(6), 59-61. https://doi.org/11.1109/MPE.2016.2591760

Horton, R., D. Boteler, T.J. Overbye, R. Pirjola, R.C. Dugan, (2012). A test case for the calculation of geomagneitcally induced currents. IEEE Transaction on power delivery, vol. 27, N.4., pp. 2368-2373.

Trichtchenko, L. D., H.-L. Lam, D. H. Boteler, R. L. Coles, J. Parmelee. Canadian space weather forecast services, Canadian Aeronautics and Space Journal August 2009, 55(2):107-113, 2009, https://doi: 10.5589/q09-013

Molinski, T.S. (2002). Why utilities respect geomagnetically induced currents. Journ. of Atm. and Solar-Terrestrial Physics, v64, #16, pp1765-1778. https://doi.org//10.1016/S1364-6826(02)00126-8

NERC Implementation Plan, Project 2013-03 Geomagnetic Disturbance Mitigation Reliability Standard TPL-007-2. (2018); available at: https://www.nerc.com/pa/Stand/Pages/Project-2013-03-Geomagnetic-Disturbance-Mitigation.aspx

Simpson, F., and K. Bahr (2005), Practical Magnetotellurics, 1-254 pp. Cambridge University

Press, Cambridge, UK.

Trichtchenko,L.and D.H.Boteler, “Modeling geomagnetically induced currents using geomagnetic indices and data”, IEEE Trans. on Plasma Sci., v 32 N4,1459-1467, 2004]

Trichtchenko, L. and D.H. Boteler, Response of Power Systems to the Temporal Characteristics of Geomagnetic Storms, pp. 390-393, 1-4244-0038-4 2006, IEEE CCECE/CCGEI, Ottawa, May 2006.

Trichtchenko, L., Fernberg, P. A., Boteler, D. H., (2019a). One-dimensional layered Earth models of Canada for GIC applications, part 1: General description. Geological Survey of Canada, Open File 8594, 2019, 66 pages, https://doi.org/10.4095/314804 (Open Access)

Trichtchenko, L., Fernberg, P.A., and Danskin, D.W., 2016. Geoelectric field modelling for Canadian Space Weather services; Geological Survey of Canada, Open File 8115, 140 p. doi:10.4095/299116

Weaver, J. T.: Mathematical methods for geo-electromagnetic induction, Research Studies Press LTD, Taunton, Somerset, England, 1994.